Review of “Impacts of orography and urbanization on extreme precipitation event in Beijing during 2023” by Haobo Cui et al.

General Comments

This manuscript investigates the impacts of orography and urbanization on the extreme precipitation event in Beijing during July 29 - August 2, 2023, using WRF model sensitivity experiments. The topic is timely and relevant given the increasing frequency of extreme weather events in urban areas with complex topography. The authors employ a reasonable experimental design with three scenarios to isolate effects of terrain and land use. However, several significant concerns need to be addressed before the manuscript can be considered for publication. The issues are substantial but addressable. Therefore, major revisions are recommended.

Response: We highly appreciate you for your thorough review and constructive comments, which significantly improve the quality of our manuscript. We have carefully considered all comments and have made the following changes.

(1) The evaluations of model simulation with meteorological observation were complemented and the quantitative statistics were listed to make the results more convincing.

(2) The water vapor budget was quantitatively assessed to improve the physical mechanism.

(3) The methodological choices were better justified to enhance the scientific contribution.

(4) More discussion including the ensemble simulation, the uncertainty quantification and the important limitations of our study were added.

We have also checked the English texts carefully and corrected the grammatical errors through the manuscript. Below we indicate the comments and use blue font for our responses. We hope the following point-to-point response could address your concern.

Major Comments

1. One of the concerns is the substantial precipitation overestimation in the southwestern mountainous region, which is precisely the area of primary scientific interest. The model simulates over 800 mm while CMORPH shows less than 700 mm (lines 276-278). This raises fundamental questions about whether the diagnosed physical mechanisms are correctly represented in the model. When the model gets the magnitude wrong in the key region, how confident can we be that it correctly represents the processes causing those differences between sensitivity experiments?

Response: Thanks for your comments. Previous studies have recognized that there are large uncertainties in precipitation observations and satellite-derived products across regions with complex terrain (Zhou et al. 2008, Yu et al. 2009, Yu et al. 2025), a concern our research also acknowledges. However, this study focused on evaluating the model's ability to reproduce the spatial distribution characteristics of precipitation and the comparison among different experiment schemes. Although the control experiment exhibits a certain wet bias over the southwestern mountainous area, all sensitivity experiments employ exactly the same dynamical and physical configurations. Since the CMORPH data is not directly observed, the model simulations were further validated using meteorological observation from 27 stations in the revised version. It was found that, the maximum observed precipitation is 772.2 mm, which was comparable with the simulation results. The average precipitation amount 237.0 mm, and the simulated value on the grid where the station located in is 228.4 mm. Therefore, the magnitudes were analogous between model simulation and observation in the target area.

The authors should provide comprehensive quantitative validation metrics including RMSE, bias, and correlation coefficients for different sub-regions, not just qualitative, descriptive comparisons. More importantly, they need to explicitly discuss how this bias might affect their interpretation of the sensitivity experiments. Does the overestimation suggest the model is too sensitive to orographic forcing? If so, might

the diagnosed “impacts” of terrain removal be exaggerated? Additionally, while the authors note limitations in mountain station data, surely some station data from the plains areas were available and could strengthen the validation.

Response: To evaluate the simulation accuracy of the WRF model across different study areas (D04 in the manuscript), it is divided into mountain area (where terrain height greater than 100 m) and plain area (where terrain height smaller than 100 m). The Figure 4 in the initial version was reproduced with the scatter plots shown separately for the mountain and plain areas. The quantitative statistics were listed in Table 2 in the revised version. The more explanations are added as follows.

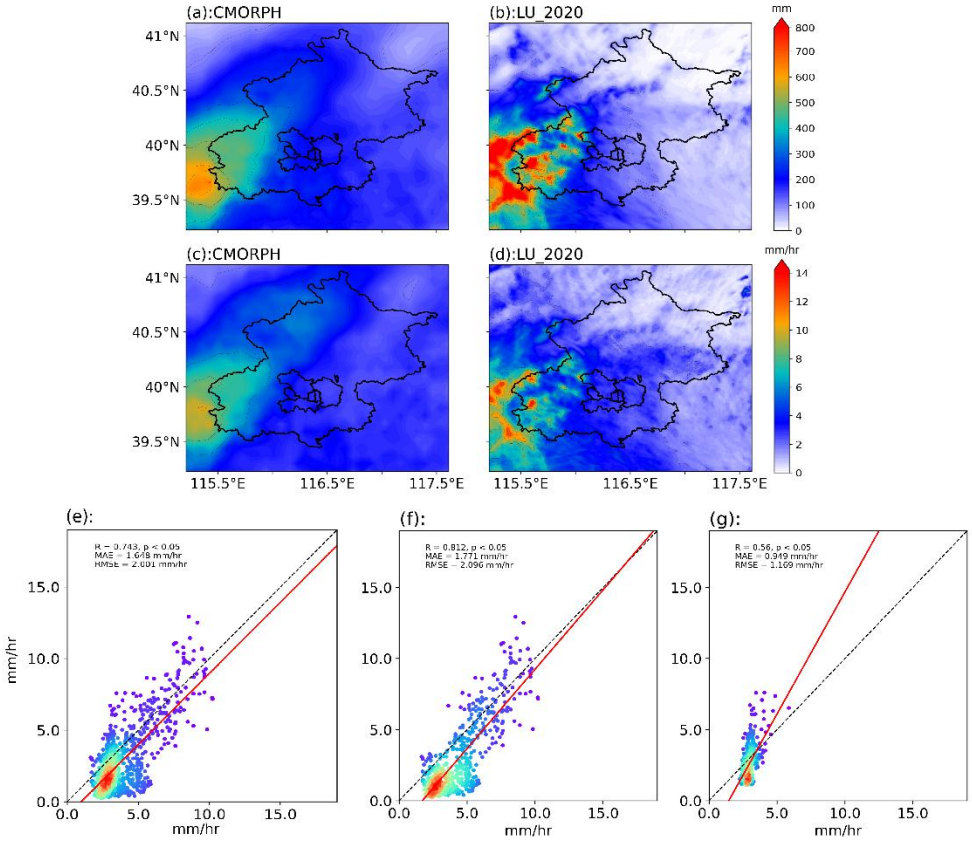

Figure 4: Comparison of simulated and observed precipitation: (a)–(b) accumulated precipitation for CMORPH and LU_2020, respectively; (c)–(d) average precipitation intensity for CMORPH and LU_2020; and (e) scatter plots for the precipitation intensity for CMORPH in x axis and LU_2020 in y axis, while the red line represents the linear regression; (f) and (g) representing area where terrain height greater than 100 m and smaller than 100 m.

Table 2: Statistics of the precipitation intensity between simulations and CMORPH data.

	R	RMSE	MAE
All	0.743	2.001	1.648
Mountain	0.812	2.096	1.771
Plain	0.560	1.169	0.949

It shows that, the correlation coefficient (R = 0.56) of the plain areas shows a smaller value compared with the two aforementioned datasets (R = 0.74 and 0.81, respectively). For the result of MAE and RMSE, the statistics in the plain areas are significantly superior to those in the mountainous areas and the entire study region. This may be due to that there are more stations in the plain areas, and the precipitation is smaller than mountain areas. We admitted that there are limitations of regional models for simulations with removed orography may influence the meteorological boundary conditions (Babaei et al. 2021). However, the terrain-removal experiment adopted in this study follows the idealized sensitivity framework widely used is used to investigate the impact of orographic effects (Boos and Kuang 2010, Arushi et al. 2017, Babaei et al. 2021). In addition, we only removed the topographic elevation without altering any other variables in LU_nohgt experiments. Thus, the impacts of orographic may introduce errors but the impacts are limited. We also explored the scheme with setting the terrain above 0 m to exactly 0 m, to detect the simulation uncertainty in terrain removal schemes. Please our response to your major concern 3.

2. Throughout the manuscript, results are presented with spurious precision and no uncertainty estimates. For example, stating that “accumulated precipitation was 229.42 mm higher” (line 301) implies 0.01 mm accuracy that simply does not exist in numerical weather prediction. These are not measurements but model outputs from a single realization with one choice of parameterizations.

Response: Thanks for your comments. In this study, the cumulative precipitation was actually the mean obtained by averaging the grid-point precipitation over the study area. However, we indeed ignored the fact that the precipitation values simulated by the model are accurate to 0.1 mm. In the revised version, we have corrected the descriptions related to average precipitation to enhance the precision of expressions.

The entire attribution analysis rests on differences between model experiments, yet there is no assessment of whether these differences exceed natural variability or model noise. What if you ran the simulation starting 6 hours earlier? What if you used different physics schemes? The differences might vary substantially. Without any ensemble members or uncertainty quantification, readers cannot assess the robustness of the conclusions.

The authors acknowledge this limitation briefly in the discussion but do not adequately address its implications. Even a small ensemble of 3-5 members with perturbed initial conditions would greatly strengthen confidence in the results. Additionally, the language throughout should be more cautious, using phrases like "the model suggests" rather than definitive statements about impacts.

Response: We admitted that, physical parameterization options have significant influences on precipitation simulations, not only for the magnitude and duration, but also for spatial and temporal distribution. The parameterization method adopted in this study had also been used in other studies about urban extreme precipitation events (Ryu et al. 2016, Wang et al. 2018, Luo et al. 2023, Wang et al. 2023, Xian et al. 2023), which can partly can prove the rationality of this study. Following your suggestion, the model uncertainty was further accessed using an ensemble simulation of LU_2020 scheme, where are originated from 10 ensemble members of ERA5. They provide estimates of the short-range forecast uncertainty, and can be considered to represent the evolution of the errors in the high-resolution component of ERA5 (Hersbach et al. 2020). The results were shown in Supplementary Figure S4 and the following tests were added in the revised version.

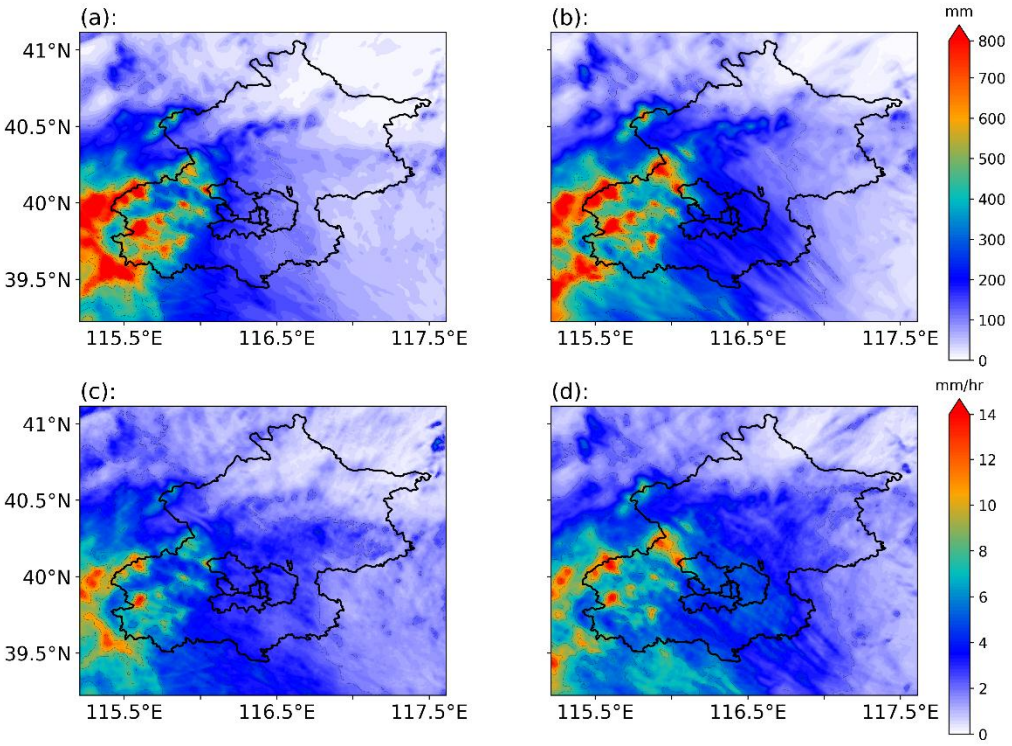

Figure S4: Comparison between simulated results of the events. (a), (b) represents the accumulated precipitation amount of LU_2020 experiment and 10 members ensemble mean, while (c), (d) represents the corresponding intensity simulation, respectively.

The results show that there is slightly difference between the ensemble mean simulation and our experimental results (Figure S4). Statistically, the average precipitation intensity is 3.6 mm/hr for LU_2020 scheme and 4.1 mm/hr for the ensemble mean. The RMSE and MAE of precipitation intensity is 1.17 mm/hr and 0.86 mm/hr for the two simulation results and the correlation coefficient is 0.90. Therefore, the experimental scheme and simulation results in this study are convincing. We have added this discussion in the revised version.

Additionally, we have revised the language throughout the manuscript, to be more cautious as you suggested.

3. The choice to set all terrain above 100 m to exactly 100 m (lines 201-204) creates an artificial plateau. This decision appears arbitrary and is inadequately justified. Why 100 m specifically? A supplementary experiment with completely flat terrain would help clarify whether results depend on this somewhat arbitrary choice.

Response: Thanks for your comments. In our manuscript, the choice of removing the terrain with an elevation above 100 meters to ensure that the terrain in other regions would not be affected while eliminating the terrain of the Taihang Mountains and the Yanshan Mountains and exploring the impact during the precipitation event. Similar experimental design had been used in several other researches (Boos and Kuang 2010, Insel et al. 2010, Saurral et al. 2015). To detect the influence of the terrain removal operation, the experiment was repeated after removing all the terrain in the entire research area to explore the simulation of completely flat terrain. The experimental results were shown in Supplementary Figure S5 as follows.

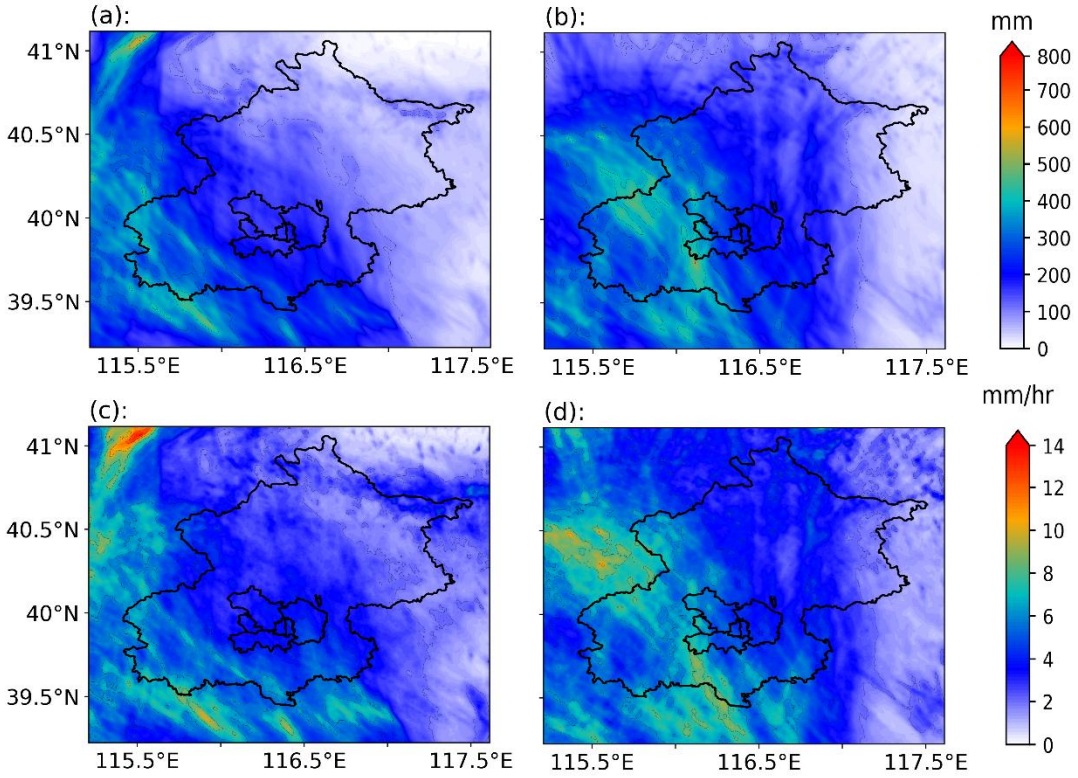

Figure S5: Accumulated precipitation and intensity distribution of the event. (a, b) represents the accumulated precipitation amount of 100 m removal experiment and 0 m removal experiment, while (c, d) represents the corresponding precipitation intensity, respectively.

It can be seen from Figure S5 that the spatial patterns of precipitation are similar for the schemes of 100 m and 0 m removal experiment. The maximum precipitation center of 0 m removal experiment shifts eastward, which is mainly because the flatter terrain enhanced the northward transport of water vapor and further slowed the

dissipation of the remnant low of Doksuri. It therefore increases the precipitable water over the region and leads to a more intense precipitation event. Statistically, the mean precipitation intensity is 4.2 mm/hr and 4.7 mm/hr for the 100 m and 0 m removal experiment, respectively. The RMSE and MAE of precipitation intensity is 1.54 mm/hr and 1.17 mm/hr between these two schemes and the correlation coefficient is 0.74. The results proved the strong relationships between the precipitations from 100 m and 0 m removal experiment schemes, which may apply to other precipitation-related variables. We have added this discussion in the revised version.

4. While the manuscript presents extensive diagnostics, the analysis often remains qualitative when quantitative assessment is needed. The moisture budget analysis (Figures 8-9) shows flux magnitudes, but nowhere do the authors calculate the net moisture convergence. How much moisture actually enters through the southern boundary? How much exits through the northern boundary? What is the net convergence, and how does it relate to the precipitation amount?

Response: Thanks for your comments. We realized that the results can be more convincing, with the quantitative calculation of moisture budget analysis. Following your suggestion, the quantitative water vapor fluxes were listed in Table 3.

Table 4: The water vapor flux (kg/(m s)) during each period for different schemes.

Time	Scheme	North	South	Zonal	East	West	Meridional	Net
T1	LU_2020	58.63	-19.52	39.11	130.50	-100.61	29.89	69.00
	LU_nohgt	78.89	-83.09	-4.20	141.79	-110.93	30.86	26.66
	LU_nourb	55.42	-22.42	33.00	133.97	-94.19	39.78	72.78
T2	LU_2020	146.94	-109.39	37.55	146.05	-160.02	-13.97	23.58
	LU_nohgt	222.99	-146.99	76.00	176.09	-199.31	-23.22	52.78
	LU_nourb	152.31	-113.83	38.48	139.02	-150.29	-11.27	27.21
T3	LU_2020	199.32	-169.36	29.96	71.65	-95.36	-23.71	6.25
	LU_nohgt	228.22	-237.85	-9.63	32.12	-0.69	31.43	21.80
	LU_nourb	206.16	-160.40	45.76	74.65	-64.38	10.27	56.03

In addition, in order to enable readers and reviewers to more clearly discern the variations in moisture transport from different boundaries, The corresponding figures (Figures 8 and 9 in the initial version) was reproduced. In these new figures, positive moisture flux denotes the transport of water vapor into the region, whereas negative

values indicate the export of water vapor from the region. The corresponding texts were revised to make the results quantitatively explicit.

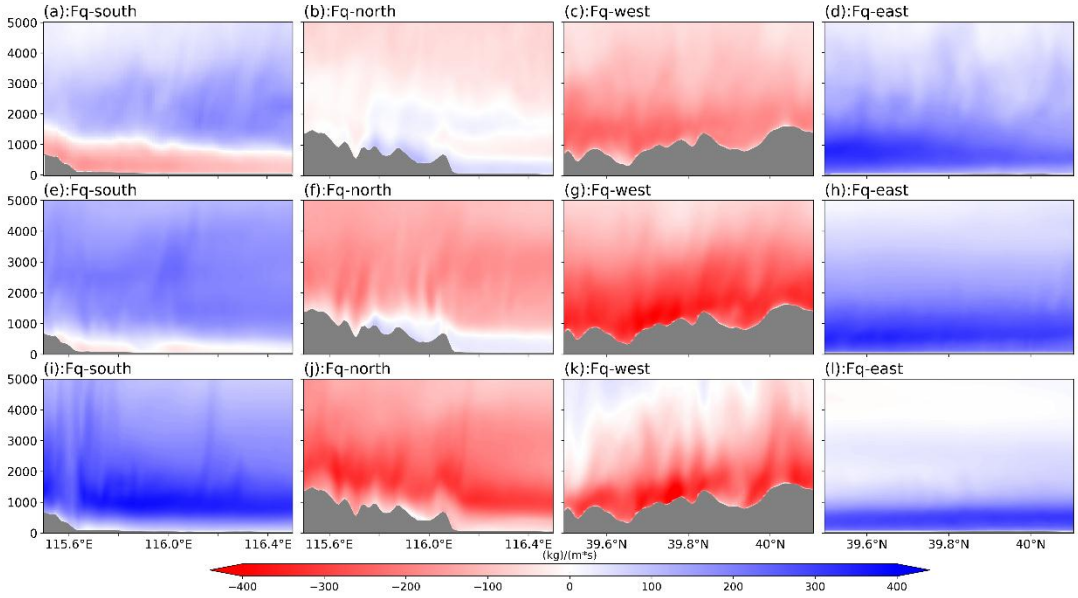

Figure 8. Distribution of water vapor flux magnitude in the LU_2020 scheme across latitude-height/longitude-height coordinates of RegP. Figures show the water vapor flux magnitude for time periods T1 (a – d), T2 (e – h), and T3 (i – l), with fluxes from the south (a, e, i), north (b, f, j), west (c, g, k), and east (d, h, l). Positive and negative water vapor flux values correspond to input and output water vapor flux relative to RegP.

Figure 8 shows the magnitudes of the water vapor flux at the four boundaries of region RegP for LU_2020. An increase in net moisture convergence during each period leads to higher precipitable water over the region, which in turn provides more favorable conditions for precipitation over study region. Specifically, the moisture inflow across the southern boundary (Figure 8a, e, i) and the eastern boundary (Figure 8d, h, l) represents meridional and zonal sources of water vapor entering the region. The outflow across the northern boundary (Figure 8a, e, i) and the western boundary reflects the moisture exported from the region. The difference between the inflow and outflow moisture flux indicates net moisture income in each time period (shown in Table 2).

During period T1, about 49.58 kg/(m s) water vapor was transported southward at lower latitudinal levels along the southern boundary, while it was transported northward at high latitudes (in total 58.63 kg/(m s) northward). As the Taihang

Mountains extend in a southwest-northeast direction in the study area, the eastern zonal airflow (in total 130.50 kg/(m s)) blocked by the Mountainous area and shifted southward which explained why water vapor was transported southward in northern boundary. Overall, at T1, the moisture input into the region was dominated by zonal water vapor transport. Although the meridional transport contributed a relatively large amount of moisture inflow, its substantial outflow resulted in a comparatively smaller net contribution to the regional moisture budget.

During periods T2 and T3, the water vapor flux distributions were similar between the two periods, while the magnitude of water vapor decreased in period T3 (from 23.58 kg/(m s) to 6.25 kg/(m s)). Although the zonal water vapor transport increased to some extent, the total moisture inflow during the two periods remained comparable. Meridionally, the eastward water vapor flux also decreased from T2 to T3 (from -13.97 kg/(m s) to -23.71 kg/(m s)). In addition, the water vapor transport during T3 became more concentrated in the lower layers which indicate the contribution of low-level water vapor transport to the precipitation process. Compared with that in T1, the northward water vapor flux at the southern boundary was significantly increased in T2 and T3. As in T2 and T3 periods, the northwestward transport increased and led to strong uplift motion in the mountainous area. Consequently, the mountainous areas may have been more prone to intense convective weather events due to the sufficient water vapor and air uplift during T2 and T3.

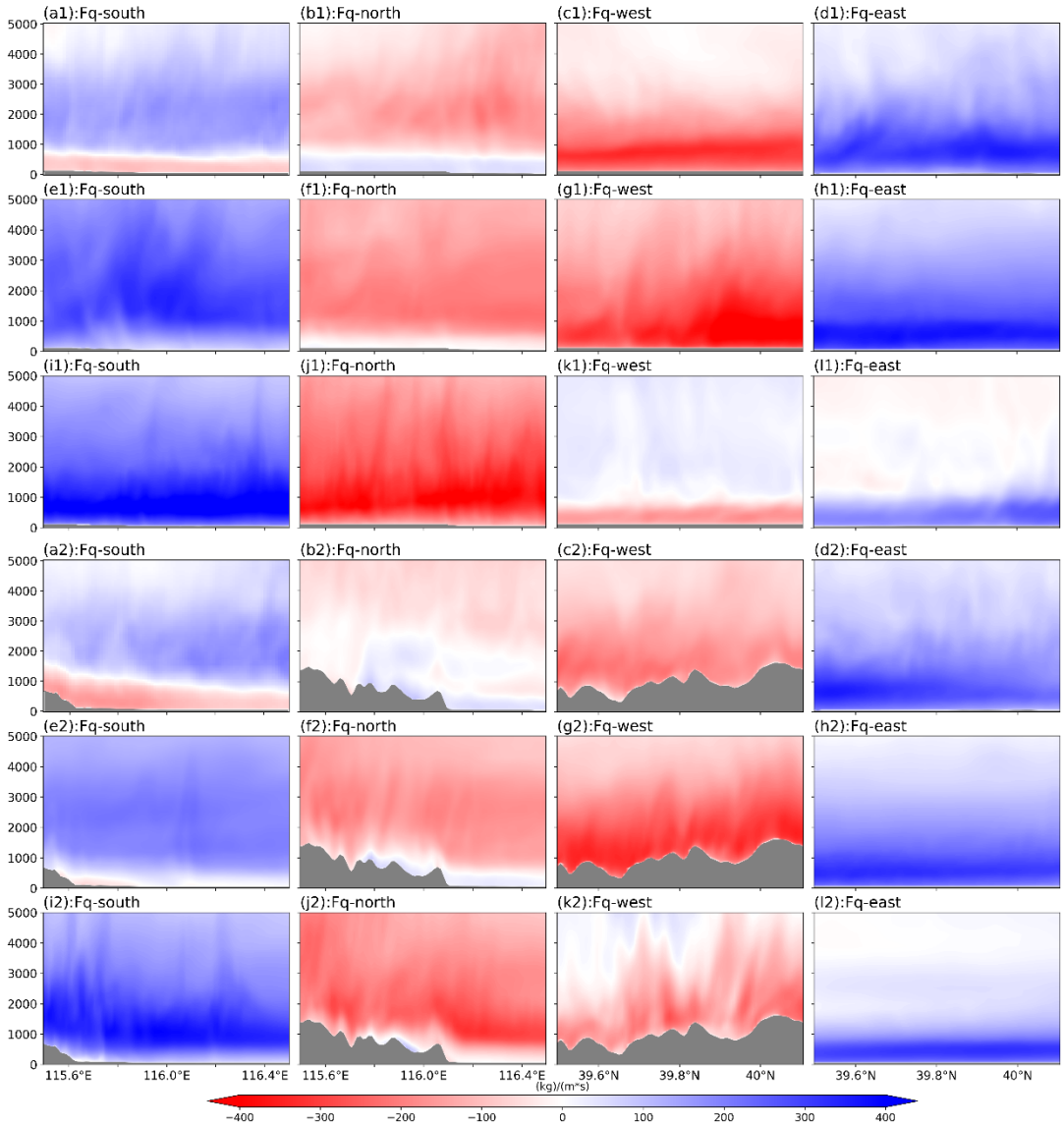

Figure 9. Water vapor fluxes as shown in Figure 8, where a1 – l1 depict the magnitude of the water vapor flux from four directions in the LU_nohgt scheme, and a2 – l2 depict the magnitude of the water vapor flux from four directions in the LU_nourb scheme.

Orographic height significantly impacted water vapor flux transport, as shown by the differences in the water vapor distribution between LU_2020 (Figure 8(a – l)) and LU_nohgt (Figure 9(a1 – l1)) and their corresponding water vapor flux transport in table 2. From a zonal perspective, orography considerably influenced the water vapor distribution within RegP. Due to orographic effects, water vapor was lifted and its northward transport was prevented, statistically reduced about 63.57 kg/(m s) in the LU_2020 (Figure 9 a1, e1, and i1), which also increased the total amount of zonal water vapor flux in LU_2020. From meridional perspective, the meridional water

vapor flux output from western boundary substantially decreased during the whole period (49.41 kg/(m s) to 79.38 kg/(m s)), resulting in a noticeable rise in the water vapor content in the entire region. Furthermore, the easterly winds were blocked and diverted by the orographic effect of the mountains to the west of Beijing, which also leads to a modest increase in the magnitude of the southward water vapor flux at the southern boundary in the lower atmospheric layers.

The impacts of the urbanization on water vapor transport are shown in Figure 9(a2 – l2). There was no significant difference between LU_2020 and LU_nourb in water vapor flux during periods T1 and T2 as the difference between net convergence is smaller than 10 kg/(m s), but during period T3, the differences mainly appeared at the western boundaries of region RegP. At the western boundary, the westward water vapor flux was 30.98 kg/(m s) higher compared with that in LU_nourb (Figure 9(k2)). These differences of moisture flux between different schemes were mainly due to wind speed in lower troposphere. As urban land use can influence local atmospheric circulation, such strong ascent induces horizontal convergence and a subsequent conversion of horizontal momentum into vertical motion. Such momentum redistribution can reduce the horizontal wind speed, particularly within the convectively active region, leading to a reduction in moisture flux across the western and northern boundaries.

Additionally, the authors should track the low-pressure center explicitly, show geopotential height evolution, and calculate steering flow to demonstrate the blocking mechanism quantitatively. Similarly, the subtropical high is mentioned repeatedly as an important factor but is never analyzed with actual diagnostics of its position and strength.

Response: Thanks for the comments. We have shown the synoptic circulation at key time points in Figure 3 in the manuscript, which may be insufficient to capture its evolution. Following your suggestion, the temporal resolution has been refined and the circulation is newly provided illustrate the evolution of the weather system in the reproduced Figure 3 in the revised version. The corresponding results are revised as

follows.

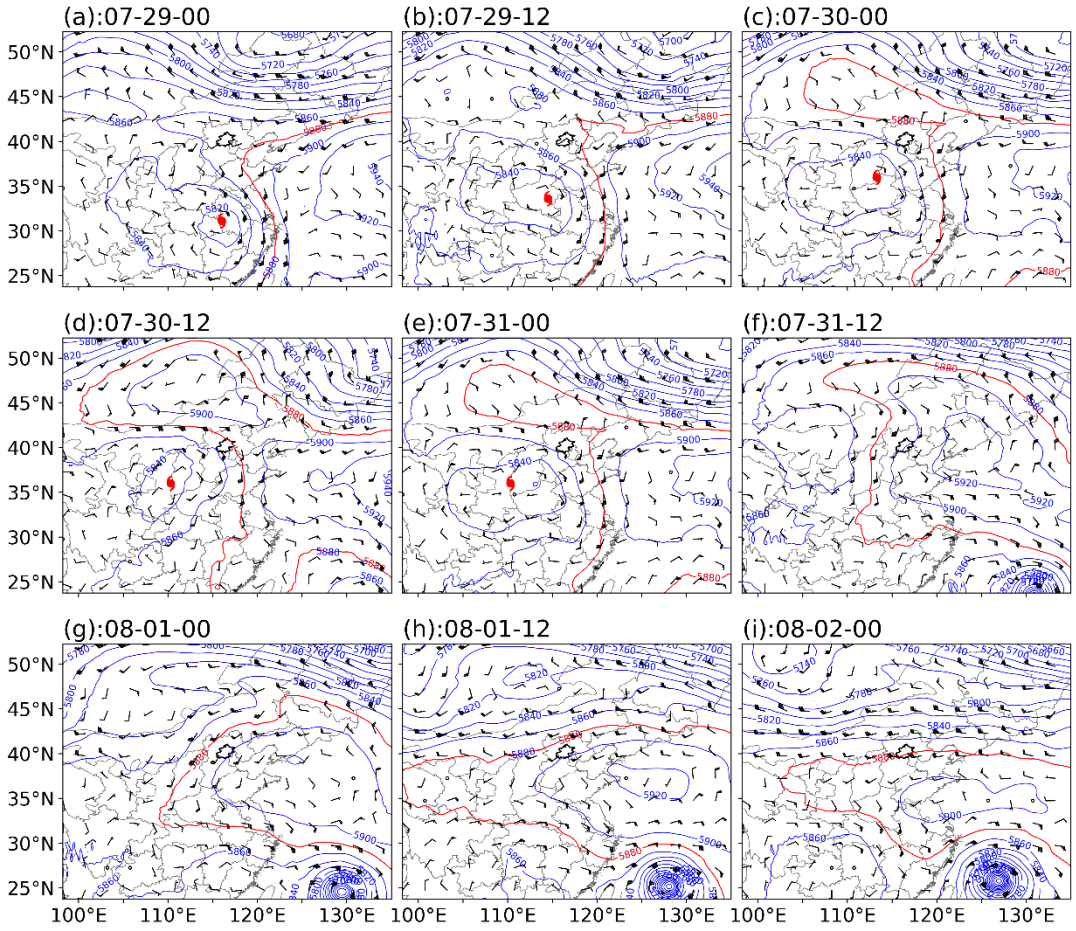

Figure 3: 500hpa circulation pattern for the precipitation event (source: ERA5). The blue solid lines represent geopotential height contours; the red solid contours represent position of subtropical high; the typhoon symbols in (a) - (e) represent residual circulation center of typhoon Doksuri.

As shown in Figure 3, on 29 July the remnant low of Typhoon Doksuri maintained considerable intensity at the 500-hPa level, with its center located near 112 °–114 °E, 32 °–34 °N. At this time, the main body of the Western Pacific Subtropical High was situated along the eastern coastal region of China and the adjacent seas, with the westernmost position of the 5880-gpm geopotential height contour around 118 °E, indicating a limited westward extension. The Beijing area was primarily located within the weakly influenced northwestern periphery of the Western Pacific Subtropical High, where low-level moisture transport was relatively weak and no significant heavy precipitation had yet developed.

By 30 July, the Western Pacific Subtropical High had extended westward, with the

5880-gpm contour reaching approximately 105°–110°E and stretching northward to Mongolia, thereby establishing a relatively stable high-pressure ridge to the north of the Doksuri remnant low and forming a typical blocking circulation pattern. Under these conditions, the center of the remnant low oscillated slightly within 112°–115°E and 33°–35°N, exhibiting a displacement of less than 2° in latitude and 3° in longitude over 48 hours, indicative of a pronounced quasi-stationary state that persisted until around 1200 UTC on 31 July. During this period, Beijing was located between the southern of the blocking high and the northern side of the remnant low, a configuration favorable for sustained southerly to easterly flow and continuous moisture transport toward Beijing and its surrounding regions under a supportive large-scale circulation background.

After 1200 UTC on 31 July, the remnant low of Doksuri gradually weakened and shifted slightly westward, while the blocking high began to decay. Meanwhile, Typhoon Khanun over the offshore waters of China (see the lower-right panels of Figure 3f–i) established a strong cyclonic circulation on its northwestern side, further enhancing moisture transport into North China and markedly increasing precipitable water, thereby triggering the heavy precipitation event between 1200 UTC on 31 July and 0000 UTC on 1 August. After 1 August, the Western Pacific Subtropical High intensified further and continued its westward extension, with the 5880-gpm contour maintained west of approximately 108°E. The western ridge of the strengthened Western Pacific Subtropical High subsequently blocked the moisture transport pathway from Typhoon Khanun toward North China, leading to a pronounced reduction in regional moisture inflow and the gradual weakening and termination of the precipitation process.

5. The discussion section does not adequately address important limitations or place the results in broader context. The authors note that their precipitation distribution differs from multi-year averages found in previous studies (lines 680-695) but do not adequately explain what makes this event anomalous or how that affects generalizability. Are the topographic and urban effects similar in other Beijing

extreme rainfall events, or is this case unusual? Such context would help readers understand what aspects of these findings might apply more broadly.

Response: Thanks for your comments. We admitted that the interpretation of this section was not sufficiently clear and caused confusions. In the revised version, we address the important limitations of this study and added more discussions to place the results in broader context

Urban effects identified from climatological statistics represent mean-state responses, while extreme-event precipitation is often governed by nonlinear, event-specific dynamical forcing, and that may cause precipitation distribution pattern comparing to the multi-year average (Liu and Niyogi 2019). In addition, as shown in the results, the water vapor transport of this precipitation event was mainly dominated by the southeasterly water vapor flux governed by the large-scale circulation, which thus triggered precipitation in the southwestern piedmont area of the Taihang Mountains and led to the aforementioned differences. Although precipitation also occurred in the northwestern region, its overall intensity was significantly weaker than that in the southwestern region, which is also the reason why this precipitation event is distinct from other precipitation events.

Orography and urbanization exert a significant influence on precipitation in Beijing, particularly in the occurrence of extreme precipitation events. Previous studies have analyzed the role of topographic factors in other precipitation events over the Beijing region. For the extreme precipitation event occurred on 21 July 2012, the precipitation event was mostly generated by convective cells that were triggered by local topography and then propagated along a quasi-stationary linear convective system (Zhang et al. 2013). The effects of urbanization can also be found in single cases. As differences can be found in climatological versus case-study based assessments (Liu and Niyogi 2019). According to analyses of multiple extreme precipitation events in Beijing in recent years, by applying METRAS model in Beijing region, urbanization reduces rainfall in the urban area and increases rainfall downwind of the city, while in some cases, larger percentage of sealed area could give rise to the heavier precipitation or extreme rain events(Liu et al. 2021). As different types of

precipitation or different weather conditions can lead to variable and complex precipitation‐elevation relationships even along the same slope (Houze Jr. 2012, Gnann et al. 2025), while urban effects of each event should be analyzed independently (Liu et al. 2021). This precipitation event is somewhat representative; however, for precipitation events under different initial conditions, further investigation is needed.

Aerosols are acknowledged as potentially important but the complete absence of aerosol effects in the experiments is not adequately justified. Either the authors should explain why aerosols can be neglected for this particular event, or they should acknowledge this as a significant limitation that could be affecting their results, particularly for the urban impact attribution.

Response: Thanks for your comments. Aerosols have a significant impact on the weather in urban areas, especially on extreme weather events. However, in this manuscript, the focus is mainly on the impact of the natural factors, especially underlying surface on precipitation event. Aerosols are largely attributed to anthropogenic factors, therefore are not involved in this study and will be considered in future research.

Minor Comments - - - - -

The introduction provides good context but has some redundancy

Response: We have optimized the introduction section of the manuscript and made the corresponding revisions in the revised version.

Unclear phrasing: “The setting of altitude in the numeric model” (line 73)

Response: It has been revised to “The altitude used in the numeric model”

Several methodological choices need better justification, e.g. the upper boundary at 50 hPa and the assimilation coefficient. Are these values standard, or were they optimized for this case?

Response: Thanks for your comments. The reason why we configure the upper boundary at 50hPa is to resolve the vertical structure of the subtropical high and upper-level jet streams while minimizing spurious wave reflection near the upper boundary. The value is standard and can be seen in other researches on extreme precipitation events (Wang et al. 2018, Yu et al. 2024, Pei et al. 2025).

The cut-off wave number is selected as 3 is because the zonal and meridional length of the study region is about 3000 km ×3000 km. As the length-scale is more accurate at 1000 km (Gómez and Miguez-Macho 2017, Kukulies et al. 2023), it is convincing for cut-off wave number selected in this study. The assimilation coefficient is selected as $3\times10^{-4}s^{-1}$ in regional climate study as mentioned in previous research (Liu et al. 2012, Holst et al. 2016, Pei et al. 2025).

We have added these references in the method section of the revised version.

The use of MODIS 2020 land cover for a 2023 event raises questions about whether significant land cover changes occurred in the interim, particularly given Beijing's continued development. This should at least be acknowledged as a potential limitation.

Response: Thanks for your comment. The reason why we used 2020 rather than 2023 land cover type is that the latest version provided by MODIS corresponds to the year 2020. We referred to the data provided by Sentinel-2 and the land cover type between 2020 and 2023 were shown as below:

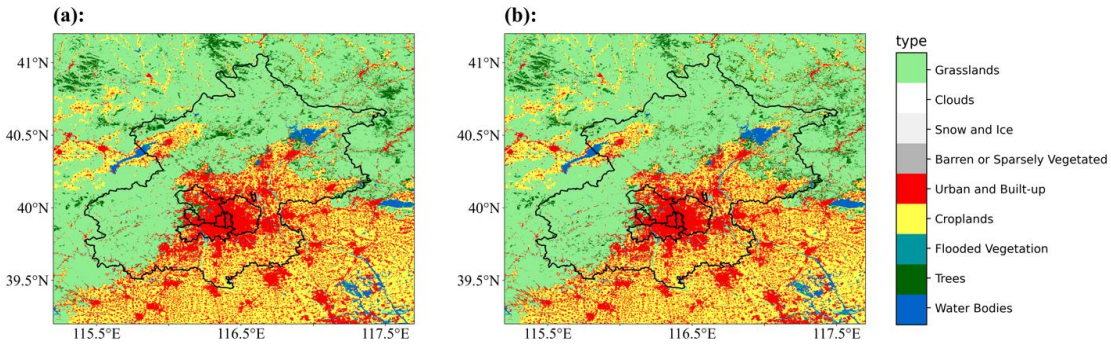

Figure R1: Comparison between land cover type in 2020 (a) and 2023 (b) in Beijing region from Sentinel-2.

From Figure R1, there are limit magnitude of land cover change between 2020 and

2023, mostly because the affections of COVID-19 pandemic restricting human activities. In addition, the MODIS adopts land cover classification of IGBP, while sentinel-2 uses different classification which cannot be input to WRF directly. Therefore, we used the data provided by MODIS in this study and we admitted that some bias can be made by land cover types. We added the corresponding discussion in the revised version.

Throughout the results, equivalent potential temperature fields are shown but rarely analyzed quantitatively. The authors should calculate and discuss gradients, baroclinic zones, and frontal features rather than just presenting the visualization.

Response: Thanks for your comments. We have recognized that presenting only the surface equivalent potential temperature is insufficient to fully illustrate the mechanism of the event occurrence and the impact of underlying surfaces. Considering that the 2-m equivalent potential temperature varies with altitude, we selected the equivalent potential temperature at 850 hPa for quantitative analysis. The results are shown in Figure 9 in the revised version and the following explanations were added.

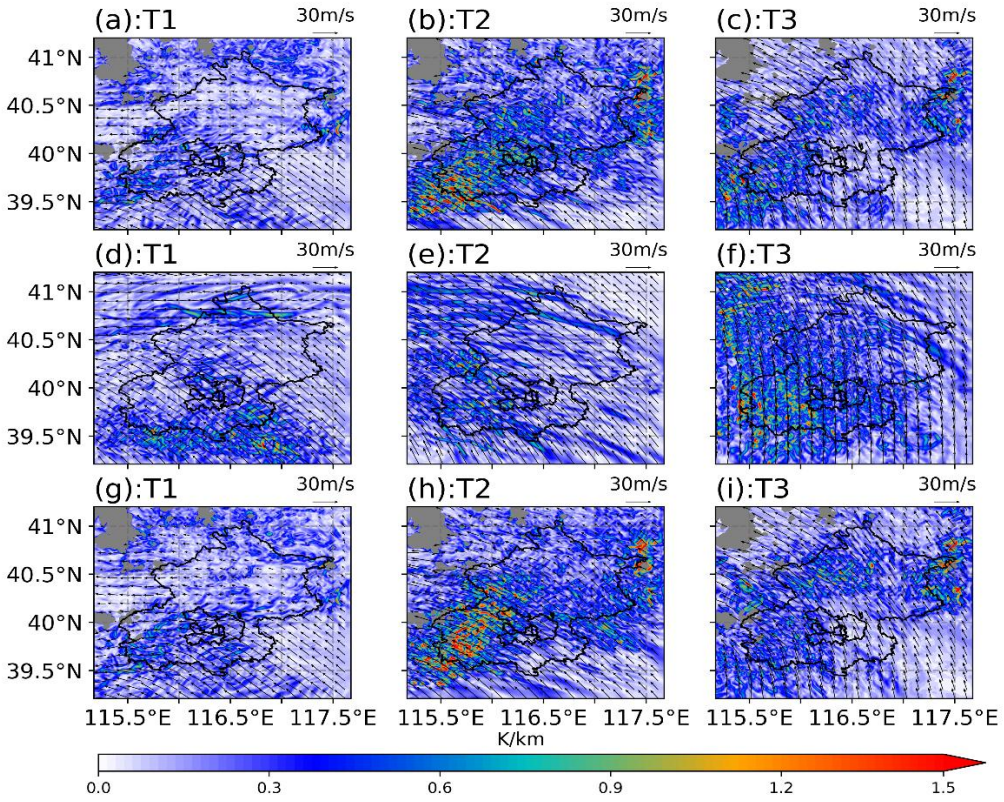

Figure 9: Gradient of equivalent potential temperature field for LU_2020 scheme (a–c), LU_nohgt scheme (d–f), and LU_nourb scheme (g–i) from 850 hPa. Three consecutive time periods were selected: T1 (a, d, g), T2 (b, e, h), and T3 (c, f, i)

The orographic lifting exerts a significant modulation on the spatial distribution of the horizontal equivalent potential temperature gradient (Figure 9). During the T1 period, the LU_nohgt scheme exhibits an eastward displacement of the maximum gradient compared with the LU_2020, accompanied by a noticeable shift in the 850-hPa wind shear location. This indicates orographic lifting alters the low-level flow and thermodynamic structure, thereby modulating the distribution of moist baroclinicity and the position of the potential frontal zone, and can provide a more favorable thermodynamic environment for convective development over the mountainous areas. During the T2 period, orographic lifting further enhances low-level moist baroclinicity and makes the high-gradient zone more continuous. Combined with the low-level wind shear, these conditions are conducive to frontogenetic processes and convective systems.

In contrast, although relatively large gradients still exist in the LU_nohgt during the

T3 period, the low-level convergence and vertical ascent are substantially weakened. It prevents the effective release of thermodynamic instability, and therefore the precipitation process consequently comes to an end. Meanwhile, the changes in urban land use also influence the precipitation intensity, especially during the T2 period. The LU_2020 scheme exhibits larger horizontal gradients over the southwestern mountainous region than LU_nourb. This indicates that urbanization can enhance low-level moist baroclinicity in this area, which is favorable for strengthening frontal structures and increasing the likelihood of intense convection precipitation.

Figure 12 with 18 panels becomes difficult to read. Consider restructuring, perhaps by moving some panels to supplementary material or combining related diagnostics.

Response: Thanks for your comments. Considering the completeness of presenting the overall experimental results, the vertical cross-sections in different directions need to be included in the manuscript. To improve the readability, we have divided the results of the terrain removal experiment and the land use modification experiment into two separate figures, while each figure was optimized.

The manuscript is generally well-written but could be more concise.

Response: Thanks for your recommendation. We have corrected the grammatical errors and revised the expressions to be more concise.

Some grammatical issues appear, e.g. “prevented the low-pressure system propagate northward” (line 23) which most likely should read “prevented...from propagating”

Response: We have checked the English texts carefully and corrected the grammatical errors through the manuscript.

Again, thanks for your thorough review and valuable comments.

The references in our response are listed as follow. Some of them are already in the manuscript, while others are newly added.

References:

1. Arushi, P. V., A. Chakraborty and R. S. Nanjundiah (2017). "Orographic control of the Bay of Bengal cold pool rainfall." *Journal of Earth System Science* **126**(8): 111.
2. Babaei, M., O. Alizadeh and P. Irannejad (2021). "Impacts of orography on large-scale atmospheric circulation: application of a regional climate model." *Climate Dynamics* **57**(7): 1973-1992.
3. Boos, W. R. and Z. Kuang (2010). "Dominant control of the South Asian monsoon by orographic insulation versus plateau heating." *Nature* **463**(7278): 218-222.
4. Gnann, S., J. W. Baldwin, M. O. Cuthbert, et al. (2025). "The Influence of Topography on the Global Terrestrial Water Cycle." *Reviews of Geophysics* **63**(1): e2023RG000810.
5. Gómez, B. and G. Miguez-Macho (2017). "The impact of wave number selection and spin-up time in spectral nudging." *Quarterly Journal of the Royal Meteorological Society* **143**(705): 1772-1786.
6. Hersbach, H., B. Bell, P. Berrisford, et al. (2020). "The ERA5 global reanalysis." *Quarterly Journal of the Royal Meteorological Society* **146**(730): 1999-2049.
7. Holst, C. C., C.-Y. Tam and J. C. L. Chan (2016). "Sensitivity of urban rainfall to anthropogenic heat flux: A numerical experiment." *Geophysical Research Letters* **43**(5): 2240-2248.
8. Houze Jr., R. A. (2012). "Orographic effects on precipitating clouds." *Reviews of Geophysics* **50**(1).
9. Insel, N., C. J. Poulsen and T. A. Ehlers (2010). "Influence of the Andes Mountains on South American moisture transport, convection, and precipitation." *Climate Dynamics* **35**(7): 1477-1492.
10. Jenney, A. M., S. L. Ferretti and M. S. Pritchard (2023). "Vertical Resolution Impacts Explicit Simulation of Deep Convection." *Journal of Advances in Modeling Earth Systems* **15**(10): e2022MS003444.
11. Jiang, L. and J. Hu (2023). "Influence of the lowest model level height and vertical grid resolution on mesoscale meteorological modeling." *Atmospheric Research* **296**: 107066.
12. Kukulies, J., A. F. Prein, J. Curio, et al. (2023). "Kilometer-Scale Multimodel and Multiphysics Ensemble Simulations of a Mesoscale Convective System in the Lee of the Tibetan Plateau: Implications for Climate Simulations." *Journal of Climate* **36**(17): 5963-5987.
13. Liu, J. and D. Niyogi (2019). "Meta-analysis of urbanization impact on rainfall modification." *Scientific Reports* **9**(1): 7301.
14. Liu, J., K. H. Schlünzen, T. Frisius, et al. (2021). "Effects of urbanization on precipitation in Beijing." *Physics and Chemistry of the Earth, Parts A/B/C* **122**: 103005.
15. Liu, P., A. P. Tsimpidi, Y. Hu, et al. (2012). "Differences between downscaling with spectral and grid nudging using WRF." *Atmos. Chem. Phys.* **12**(8): 3601-3610.
16. Luo, Y., J. Zhang, M. Yu, et al. (2023). "On the Influences of Urbanization on the Extreme Rainfall over Zhengzhou on 20 July 2021: A Convection-Permitting Ensemble Modeling Study." *Advances in Atmospheric Sciences* **40**(3): 393-409.
17. Pei, L., S.-G. Miao, X.-Y. Huang, et al. (2025). "Assessing the added value of convection-permitting modeling for urban climate research: A case study in eastern China." *Advances in Climate Change Research* **16**(1): 1-11.
18. Ryu, Y.-H., J. A. Smith, E. Bou-Zeid, et al. (2016). "The Influence of Land Surface Heterogeneities on Heavy Convective Rainfall in the Baltimore–Washington Metropolitan Area."

Monthly Weather Review **144**(2): 553-573.

19. Saurral, R. I., I. A. Camilloni and T. Ambrizzi (2015). "Links between topography, moisture fluxes pathways and precipitation over South America." *Climate Dynamics* **45**(3): 777-789.
20. Wang, J., J. Feng and Z. Yan (2018). "Impact of Extensive Urbanization on Summertime Rainfall in the Beijing Region and the Role of Local Precipitation Recycling." *Journal of Geophysical Research: Atmospheres* **123**(7): 3323-3340.
21. Wang, J., S. Miao, Q.-V. Doan, et al. (2023). "Quantifying the Impacts of High-Resolution Urban Information on the Urban Thermal Environment." *Journal of Geophysical Research: Atmospheres* **128**(6): e2022JD038048.
22. Xian, T., J. Guo, R. Zhao, et al. (2023). "The Impact of Urbanization on Mesoscale Convective Systems in the Yangtze River Delta Region of China: Insights Gained From Observations and Modeling." *Journal of Geophysical Research: Atmospheres* **128**(3): e2022JD037709.
23. Yu, H., A. F. Prein, D. Qi, et al. (2024). "Kilometer-scale multi-physics simulations of heavy precipitation events in Northeast China." *Climate Dynamics* **62**(9): 9207-9231.
24. Yu, H., A. F. Prein, D. Qi, et al. (2025). "Mesoscale Convective Systems in Northeast China From Satellite Products, Global Reanalysis, and Kilometer-Scale Modeling." *Geophysical Research Letters* **52**(11): e2024GL112349.
25. Yu, Z., H. Yu, P. Chen, et al. (2009). "Verification of Tropical Cyclone–Related Satellite Precipitation Estimates in Mainland China." *Journal of Applied Meteorology and Climatology* **48**(11): 2227-2241.
26. Zhang, D.-L., Y. Lin, P. Zhao, et al. (2013). "The Beijing extreme rainfall of 21 July 2012: “Right results” but for wrong reasons." *Geophysical Research Letters* **40**(7): 1426-1431.
27. Zhou, T., R. Yu, H. Chen, et al. (2008). "Summer Precipitation Frequency, Intensity, and Diurnal Cycle over China: A Comparison of Satellite Data with Rain Gauge Observations." *Journal of Climate* **21**(16): 3997-4010.